JGR Biogeosciences

RESEARCH ARTICLE
10.1029/2020JG005748

Key Points:
- Similar linear chlorophyll-Rubisco relationships were found between two vegetation types
- Estimation of $Vcmax_{25}$ was improved when considering chlorophyll-Rubisco relationship
- The potential of mapping $Vcmax_{25}$ with chlorophyll content was demonstrated

Supporting Information:
- Supporting Information S1

Correspondence to:
W. Ju,
juweimin@nju.edu.cn

Citation:
Lu, X., Ju, W., Li, J., Croft, H., Chen, J. M., Luo, Y., et al. (2020). Maximum carboxylation rate estimation with chlorophyll content as a proxy of Rubisco content. *Journal of Geophysical Research: Biogeosciences*, *125*, e2020JG005748. https://doi.org/10.1029/2020JG005748

Received 16 MAR 2020
Accepted 26 JUN 2020
Accepted article online 30 JUN 2020

Author Contributions:
Data curation: Jing Li
Funding acquisition: Weimin Ju
Investigation: Xuehe Lu, Jing Li, Haijing Hu
Methodology: Xuehe Lu, Holly Croft, Hua Yu
Project administration: Weimin Ju
Resources: Weimin Ju, Holly Croft, Haijing Hu
Supervision: Weimin Ju
Validation: Weimin Ju, Holly Croft, Jing M. Chen, Hua Yu, Haijing Hu
Visualization: Xuehe Lu
Writing - original draft: Xuehe Lu
Writing – review & editing: Xuehe Lu, Weimin Ju, Holly Croft, Jing M. Chen, Yiqi Luo

Maximum Carboxylation Rate Estimation With Chlorophyll Content as a Proxy of Rubisco Content

Xuehe Lu[1], Weimin Ju[1,2], Jing Li[1], Holly Croft[3,4], Jing M. Chen[1,3], Yiqi Luo[5], Hua Yu[1], and Haijing Hu[6]

[1]International Institute for Earth System Science, Nanjing University, Nanjing, China, [2]Jiangsu Center for Collaborative Innovation in Geographic Information Resource Development and Application, Nanjing, China, [3]Department of Geography, University of Toronto, Toronto, Ontario, Canada, [4]Department of Animal and Plant Sciences, University of Sheffield, Sheffield, UK, [5]Center for Ecosystem Science and Society, Northern Arizona University, Flagstaff, AZ, USA, [6]School of Life Science, Nanjing University, Nanjing, China

Abstract The maximum carboxylation rate (Vcmax) is a key parameter in determining the plant photosynthesis rate per unit leaf area. However, most terrestrial biosphere models currently treat Vcmax as constants changing only with plant functional types, leading to large uncertainties in modeled carbon fluxes. Vcmax is tightly linked with Ribulose-1,5-bisphosphate carboxylase/oxygenase (Rubisco). Here we investigated the relationship between leaf chlorophyll and Rubisco (Chl-Rub) contents within a winter wheat paddock. With chlorophyll as a proxy of Rubisco, a semimechanistic model was developed to model $Vcmax_{25}$ (Vcmax normalized to 25°C). The Chl-Rub relationship was validated using measurements in a temperate mixed deciduous forest in Canada. The results showed that Rubisco was strongly correlated with chlorophyll ($R^2 = 0.96$, $p < 0.001$) for winter wheat since the absorption of light energy by chlorophyll and the amount of CO_2 catalyzed by Rubisco are tightly coupled. Incorporating the Chl-Rub relationship into the semimechanistic model, the root mean square error of modeled $Vcmax_{25}$ was the lowest among all estimation models. The slopes of Chl-Rub relations were almost consistent in the winter wheat and temperate forest, demonstrating the potential for using leaf chlorophyll content as a proxy of leaf Rubisco in modeling $Vcmax_{25}$ at large spatial scales. We anticipate that improving $Vcmax_{25}$ estimates over time and space will reduce uncertainties in global carbon budgets simulated by terrestrial biosphere models.

1. Introduction

Currently, terrestrial ecosystems can absorb about one third of anthropogenic CO_2 emissions on average based on the estimates of terrestrial biosphere models (TBMs) (Keenan & Williams, 2018; Le Quéré et al., 2017), which are effective tools for quantifying the carbon fluxes between the atmosphere and the terrestrial biosphere. High-quality simulation of the carbon cycle process is beneficial for future climate change projection and human development (Bonan & Doney, 2018; Friedlingstein et al., 2014). However, the range of global CO_2 absorption by leaf photosynthesis (GPP) simulated by TBMs is rather broad from 112 to 169 Pg C $year^{-1}$ (Anav et al., 2015; Piao et al., 2013), with significant differences in trends and interannual variations (Li et al., 2018).

A major source of TBMs' uncertainty is attributed to an inadequate estimation of the photosynthesis rate (Bonan et al., 2011). Most TBMs estimate photosynthesis according to the Farquhar, von Caemmerer, and Berry model, based on Michaelis-Menten principles of enzyme kinetics (Farquhar et al., 1980). The process of enzyme kinetics is modeled according to leaf temperature, photosynthetic capacity, and CO_2 concentration (Kattge et al., 2009). The gross photosynthetic rate is calculated as the minimum between the CO_2 carboxylation rate and electron transport rate (Farquhar et al., 1980), where the CO_2 carboxylation rate is determined by Vcmax, which is the maximum rate of Ribulose-1,5-Bisphosphate (RuBP) carboxylation catalyzed by enzyme RuBP Carboxylase-Oxygenase (Rubisco) (Quebbeman & Ramirez, 2016). The electron transport rate is calculated with the maximum rate of electron transport (Jmax), which limits the supply of energy for carboxylation and regeneration of RuBP (von Caemmerer & Farquhar, 1981). In most TBMs, Jmax is usually calculated from Vcmax based on their linear relationship (Beerling & Quick, 1995; Walker

et al., 2014; Wullschleger, 1993). Previous studies have shown that Vcmax normalized to 25°C ($Vcmax_{25}$) not only varies with vegetation plant functional types (PFTs) but also depends on environmental factors and has significant spatial and temporal variability (Croft et al., 2017; Groenendijk et al., 2011; Kattge et al., 2009; Smith et al., 2019). However, most TBMs assume that the $Vcmax_{25}$ of the same PFT is a fixed value. And Vcmax in TBMs is the product of this fixed $Vcmax_{25}$ and environmental constrains, such as leaf temperature and soil water content, causing uncertainties in the estimation of the terrestrial carbon budget.

Previous observations showed that $Vcmax_{25}$ is correlated to nitrogen-related plant functional traits, such as leaf nitrogen and chlorophyll contents (Croft et al., 2017; Dechant et al., 2017; Houborg et al., 2013). However, these relationships are difficult to apply to different species or at large scales because the allocation of leaf nitrogen into photosynthetic enzymes and apparatus varies in response to many other biotic and abiotic drivers (Kattge et al., 2009; Quebbeman & Ramirez, 2016; Walker et al., 2014), such as leaf lifespan (Onoda et al., 2017), leaf temperature (Verheijen et al., 2013), light intensity (Hikosaka, 2014), and species (Evans, 1989). Additionally, leaf nitrogen is difficult to retrieve from remote sensing data (Knyazikhin et al., 2013), hampering the mapping of $Vcmax_{25}$ at a regional or global scale. Using a novel approach, Zhang et al. (2018) mapped regional $Vcmax_{25}$ well according to the strong linear relationship between the satellite far-red Sun-induced chlorophyll fluorescence and optimized $Vcmax_{25}$ at the seasonal scale and improved the seasonal and spatial patterns of cropland GPP estimation in the Midwestern U.S. corn belt. As a plant trait, chlorophyll content can be inverted by remote sensing data (Croft et al., 2015; Houborg et al., 2013; Xu et al., 2019). Croft et al. (2017) demonstrated that leaf chlorophyll content was a strong proxy for $Vcmax_{25}$, due to proportional allocation of photosynthetic nitrogen between Rubisco and chlorophyll for balancing light harvesting and utilization for photosynthesis. Houborg et al. (2013) used the relationship between leaf nitrogen and leaf chlorophyll to model $Vcmax_{25}$ by a semimechanistic model.

Farquhar et al. (1980) proposed the semimechanistic model, which estimates $Vcmax_{25}$ according to the Rubisco content and its turnover rate. In photosynthetic physiology, leaf Rubisco and chlorophyll contents have a close relationship. In the photoreaction of photosynthesis, chlorophyll is an important pigment in Photosystem II and Photosystem I. Under the influence of other pigments and proteins, the absorbed light energy is converted to NADPH and ATP, which are important sources of energy in the Calvin-Benson cycle (Allen, 2002). Rubisco is an important catalyst in the Calvin-Benson cycle, which catalyzes the combination of CO_2 and RuBP to form two molecules of 3-phosphoglycerate, which are converted to glucose through a series of reactions. Thus, the absorption of light energy by chlorophyll and the amount of CO_2 catalyzed by Rubisco are tightly coupled (Andersson & Backlund, 2008). Previous studies at the leaf scale also indicated that the amounts of Photosystem II (Krall & Edwards, 1992; Ou et al., 2003) and Photosystem I (Eichelmann et al., 2004) were closely related to Rubisco content. Meanwhile, the amounts of Photosystems I and II are determined by the chlorophyll content (Burns et al., 2005; Evans & Poorter, 2001). Therefore, Rubisco and chlorophyll contents should be well correlated. However, there is still a lack of observations available to study the correlation between Rubisco and chlorophyll contents and how this relationship changes in different PFTs, which is important for mapping $Vcmax_{25}$ across large spatial scales.

Therefore, this study aims at exploring the relationship between Rubisco and chlorophyll contents in different vegetation types and to provide an accurate $Vcmax_{25}$ estimation model for its mapping using remote sensing data. The specific objectives of this research are to (1) examine the relationship between the chlorophyll and Rubisco contents across different vegetation types and (2) assess the suitability of using the relationship between chlorophyll and Rubisco contents to estimate $Vcmax_{25}$.

2. Materials and Methods

2.1. Field Site Description

Field campaigns were conducted at a farmland ecosystem station in Shangqiu, Henan Province, China (34.27°N, 115.4°E). This station is a component of the national field science research network of China. It is located in a warm temperate continental climate region, which is a typical wheat growing area in China. The mean annual precipitation and temperature are 708 mm $year^{-1}$ and 13.9°C, respectively. The soil type is mainly the tidal soil developed by the Yellow River sediments. Soil total nitrogen mass fraction is

0.78 g kg^{-1}. The amounts of N, P, and K are 240 kg ha^{-1} (N), 270 kg ha^{-1}(P_2O_5), and 150 kg ha^{-1} (K_2O), respectively. The farmland is irrigated with shallow groundwater. Our observations were conducted during the winter wheat growing season from the days of the year (DOYs) 84 (March 25) to 143 (May 23) in 2018.

2.2. Biophysical Measurements

Unfolded leaves at the top of the canopy were randomly selected for destructive sampling approximately once every 10 days, from a 30 × 30 m subset area within the larger field. On each sampling date, mean values of leaf nitrogen, chlorophyll, and Rubisco were calculated from three samples.

The samples for measuring nitrogen were dried in an oven at 80°C for approximately 48 hr until a constant weight and then determined total leaf nitrogen by the Kjeldahl method (Wolf, 1982). The leaf samples were heated with concentrated sulfuric acid to decompose protein in leaves into ammonium sulfate. The digestion was distilled after adding NaOH in the Kjeldahl's trap. Distilled samples were titrated with a standard acid solution until the end point for the purpose of calculating nitrogen concentration of the leaf sample. The variations of leaf chlorophyll and nitrogen contents were examined by these measurements on each sampling date.

The leaves sampled for chlorophyll measurements were packaged in plastic sample bags and transported into an ice box immediately after collection. About half an hour later, these samples were sent to the laboratory for leaf chlorophyll measurement. In the laboratory, leaf chlorophyll was extracted into a solution with absolute ethyl alcohol and formaldehyde mixed in a volume ratio of 1:1. The absorbance of the dissolving solution was measured at 663.8, 646.8, and 480 nm using a Shimadzu UV-1700 spectrophotometer (Wellburn, 1994).

A whole leaf was needed to measure the leaf Rubisco content, as the analysis requires a sample exceeding 0.5 g fresh weight. A portable chlorophyll meter SPAD (Konica Minolta Inc., Osaka, Japan) was used to observe the SPAD values of leaves, for which Rubisco were measured. From tial to tip of one leaf, five SPAD values were measured evenly and averaged for representing the SPAD value of the whole leaf. Following Markwell et al. (1995), an exponential model was used to convert the SPAD value into leaf chlorophyll content. Parameters of the model were fitted using our 51 pairs of SPAD values and laboratory-analyzed chlorophyll content from the same leaf samples (supporting information Figure S1) collected from the winter wheat paddock. Then, the chlorophyll content converted from SPAD values was used to explore its relationship with Rubisco.

The Rubisco content of leaves was determined by the method of Makino et al. (1985, 1986). Briefly, three top unfolded leaves were collected randomly from the field sampling area. After immersion in liquid nitrogen, the samples were stored in a refrigerator at −70°C. Finally, all the samples were stored in a package filled with dry ice and transported to the laboratory for measurement. Leaves (0.5 g) were placed in a buffer solution containing 50 mM Tris-HCl (pH 8.0), 5 mM β-mercaptoethanol, and 12.5% (*v*/v) glycerol, and the extracts were centrifuged (1,500 *g*, 15 min, and 4°C). A supernatant solution was mixed with a dissolving solution containing 2% (*w*/*v*) SDS, 4% (*v*/v) β-mercaptoethanol, and 10% (v/v) glycerol. Then, the mixture was boiled in water for 5 min for protein gel electrophoresis. An electrophoretic buffer system was used with SDS-PAGE and a discontinuous buffer system with 12.5% (*w*/*v*) separating and 4% (w/v) concentrating gels. Afterward, gels were washed with deionized water several times, stained with 0.25% Commassie Blue staining solution for 12 hr, and bleached until the background was colorless. Large subunits and relevant small subunits were transferred into a 10 ml cuvette with 2 ml of formamide and washed in a 50°C water bath for 8 hr. The washed solutions were measured at 595 nm using the background gel as a blank and bovine serum albumin as the protein standard.

2.3. Measurements of Gas Exchange

Carbon dioxide response curves (A/Ci) were measured using an LI-6800 portable infrared gas analyzer (LI-COR, Lincoln, NE, USA) at the Shangqiu site. To measure more leaves on 1 day, three leaves were measured using the A/Ci response curve method, and additional three measurements were conducted using the rapid response curve method (Stinziano et al., 2017). For the A/Ci response curve, PPFD was set at 1,800 μmol m^{-2} s^{-1}, and the stepwise CO_2 concentrations were 400, 200, 100, 50, 400, 600, 800, 1,000, 1,200, 1,500, and 1,800 ppm. Before logging measurements, the temperature, relative humidity, and CO_2 concentration of the air in the chamber were set to 25°C, 75%, and 400 ppm, respectively, and the leaves were

acclimated for 30 min. For the rapid response curve, the initial environment of the chamber was similar to that used in the A/Ci response curve method except for the CO_2 concentration, which was set to 500 ppm. After leaf acclimation, logging measurements were performed during 5 min when the CO_2 concentration gradually declined from 500 to 0 ppm. A measurement with no leaf in the chamber was also performed for the algorithm of the fast response curve method (Stinziano et al., 2017). The function fitaci in "plantecophys" R package was used to estimate $Vcmax_{25}$ for both the A/Ci response curve and fast response curve methods.

The default method in the function fitaci to fit the A/Ci response curve used nonlinear regression. Each part of the A/Ci curve was not assumed to be Vcmax or Jmax in advance. The details of this method were described by Duursma (2015). Parameter values for quantum yield of electron transport (0.24 mol mol^{-1}) and controlling the shape of light response curve (0.85 unitless) were set as default values. The Kc, Ko, and Γ* at 25°C were set to 404.9 μmol mol^{-1}, 278.4 mmol mol^{-1}, and 42.75 μmol mol^{-1}, respectively (Bernacchi et al., 2001). Then, they were corrected for temperature by a built-in function in the fitaci using the Arrhenius equation. The mesophyll conductance was not considered in fitting the A/Ci curve. Therefore, the estimated Vcmax are actually apparent values (Bahar et al., 2018).

2.4. Measurements of LAI

The leaf area index (LAI) was measured by an LI-2200 plant canopy analyzer (Li-Cor, Lincoln, NE, USA) on the same days as the measurements of biophysical parameters and gas exchange. The LAI measurements were conducted shortly before sunset. During the measurements, 1 above-canopy and 10 below-canopy readings were recorded for acquiring LAI. Ten below-canopy readings were distributed evenly along two diagonals of the field square.

2.5. Calculation of Leaf Nitrogen Allocation

Nitrogen contained in Rubisco was calculated as 16% of Rubisco content (Farquhar et al., 1980). Nitrogen content in leaf chlorophyll was calculated empirically with the assumption that chlorophyll *a* and *b* contain 6.3% and 6.2% nitrogen, respectively (Hall & Rao, 1999). And nitrogen in structure and other parts was the value of the total leaf nitrogen content minus the nitrogen content in Rubisco and chlorophyll.

2.6. Modeling $Vcmax_{25}$ by Rubisco Content

Following Friend (1995), the semimechanistic model for simulating $Vcmax_{25}$ using leaf nitrogen is shown as Equation 1. $Vcmax_{25}$ is a function of the Rubisco turnover rate at 25°C, the leaf nitrogen content, and the fraction of leaf nitrogen in Rubisco.

$$V_{\max}^{25} = K_{\text{cat}}^{25} \cdot \frac{8}{550} \cdot F_{\text{LNR}} \cdot N \cdot m_{\text{n}} \cdot 6.25 \cdot 10^{6}, \tag{1}$$

where $V_{\max}^{25}$ is the $Vcmax_{25}$ (μmol CO_2 m^{-2} s^{-1}); K_{cat}^{25} is the Rubisco turnover rate at 25°C (mol CO_2 mol $sites^{-1}$ s^{-1}) and can be calculated by Equation 6; $\frac{8}{550}$ is the constant for converting from Rubisco (kg) to moles of catalytic sites on Rubisco molecules, assuming the molecular weight of Rubisco is 550 KD and one Rubisco molecule has eight catalytic sites (Farquhar et al., 1980); F_{LNR} is the fraction of leaf nitrogen in Rubisco and can be calculated using Equation 11; N is the total leaf nitrogen content (mol N m^{-2}); m_{n} is the molar mass of nitrogen (0.0140067 kg mol^{-1}); and 6.25 (kg Rubisco kg N^{-1}) is the reciprocal of 16%, which is the fraction of nitrogen in Rubisco protein (Farquhar et al., 1980). The constant of 10^6 converts units of $V_{\max}^{25}$ to μmol m^{-2} s^{-1}. Because the Rubisco content (R) (g m^{-2}) can be calculated by N, F_{LNR}, m_{n}, and the constant of 6.25 (Equation 3), Equation 1 can be rewritten as

$$V_{\max}^{25} = K_{\text{cat}}^{25} \cdot \frac{8}{550} \cdot R \cdot 10^{-3} \cdot 10^{6}, \tag{2}$$

where

$$R = F_{\text{LNR}} \cdot N \cdot m_{\text{n}} \cdot 6.25 \cdot 10^{3}. \tag{3}$$

In this study, the relationship of chlorophyll and Rubisco contents was assumed to be linear (Equation 4), and its robustness was examined using growing season measurements of winter wheat and a temperate mixed deciduous forest.

$$R = a \cdot C + b, \tag{4}$$

where C is the leaf chlorophyll content (μg m^{-2}) and a and b were fitted using our measured chlorophyll and Rubisco contents.

Thus, Equation 2 may be reformulated as follows:

$$V_{max}^{25} = K_{cat}^{25} \cdot \frac{8}{550} \cdot 10^6 \cdot (a \cdot C + b) \cdot 10^{-3}, \tag{5}$$

where K_{cat}^{25} is calculated in accordance with Eichelmann et al. (2009):

$$K_{cat}^{25} = \frac{c}{1 + d \cdot R_{mol} \cdot 8} R_{mol} = R \times 10^6 / 550,000, \tag{6}$$

where R_{mol} is the leaf Rubisco content in μmol m^{-2}, 550,000 is the molecular weight of Rubisco, and c and d are the coefficients.

In the study of Eichelmann et al. (2009), c and d in Equation 6 were set to 4.3 and 0.03, respectively, according to collected data of multiple species. However, the uncertainty of estimated K_{cat}^{25} was large (gray area in Figure S2), which indicated the c and d of different species were not the same. Therefore, we fitted these two parameters in Equation 6 with our measured wheat leaf Rubisco and K_{cat}^{25} inferred from measured $Vcmax_{25}$ and Rubisco content using Equation A1, which was derived from Equation 2. The calibrated c and d values were 7.72 and 0.04, respectively (red line in Figure S2).

2.7. Modeling $Vcmax_{25}$ by Other Plant Traits

In order to compare the performance of modeling $Vcmax_{25}$ by different plant traits, our observations in the wheat paddock were used to verify other three models estimating $Vcmax_{25}$ from chlorophyll and nitrogen contents (Croft et al., 2017; Dechant et al., 2017; Houborg et al., 2013). All tunable parameters in these models were fitted using the measurements.

Croft et al. (2017) reported a linear model estimating $Vcmax_{25}$ from leaf chlorophyll content:

$$V_{max}^{25} = a_{VC} \cdot C + b_{VC}. \tag{7}$$

Dechant et al. (2017) estimated $Vcmax_{25}$ using the following equation:

$$V_{max}^{25} = a_{VN} \cdot N_L + b_{VN}, \tag{8}$$

where N_L is the total leaf nitrogen content (g N m^{-2}).

The third model was proposed by Houborg et al. (2013), who estimated $Vcmax_{25}$ according to Rubisco content and its turnover rate. Rubisco content was empirically estimated on the basis of total nitrogen content, which was approximated from chlorophyll content. $Vcmax_{25}$ is calculated as

$$V_{max}^{25} = K_{cat}^{25} \cdot \frac{8}{550} \cdot F_{LNR} \cdot N_L \cdot 6.25 \cdot 10^6, \tag{9}$$

where N_L is the content of total nitrogen. It is estimated as

$$N_L = a_{NC} \cdot C + b_{NC}. \tag{10}$$

The term $F_{LNR} \cdot N_L$ in Equation 9 indicates leaf Rubisco content. F_{LNR} is the fraction of nitrogen allocated into Rubisco and inversely correlated with the content of total nitrogen (Houborg et al., 2013):

$$F_{LNR} = (a_{RN} + b_{RN}/N_L) \cdot 0.16. \tag{11}$$

The values of a_{RN} and b_{RN} fitted using our observations of Rubisco and total nitrogen contents are 1.8351 and −1.5075, respectively (Figure S4).

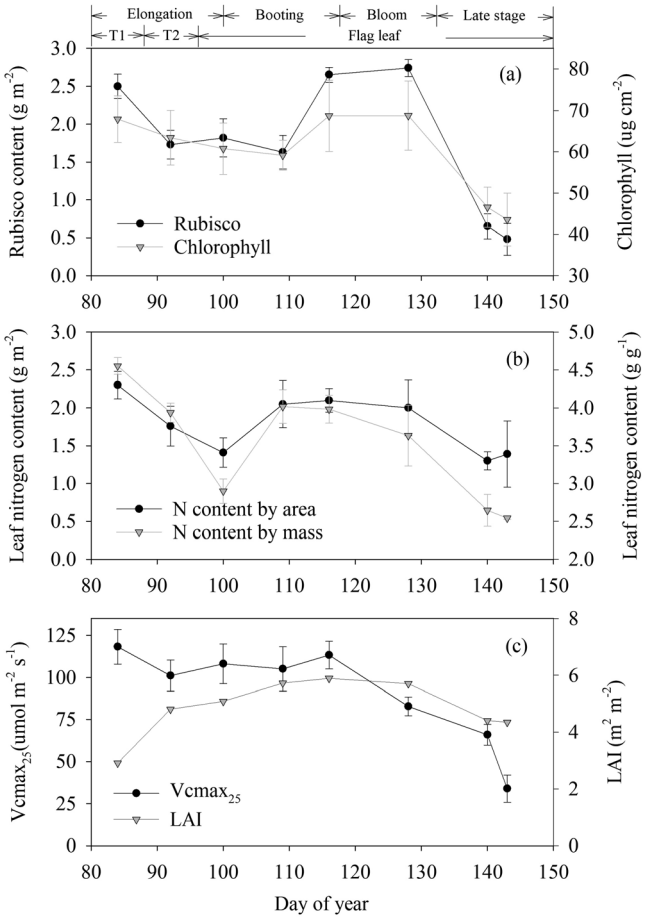

Figure 1. Seasonal variations in (a) leaf Rubisco and chlorophyll contents, (b) leaf nitrogen content, and (c) $Vcmax_{25}$ and LAI for winter wheat in 2018. Before the observation of the flag leaf, the new top leaves (T1 and T2) that grew continuously were measured in the growing stage of elongation.

2.8. Relationship Between Chlorophyll and Rubisco in a Temperate Mixed Deciduous Forest

Croft et al. (2017) reported seasonal measurements of $Vcmax_{25}$ and chlorophyll content in a temperate mixed deciduous forest located in southern Ontario, Canada (44.32°N, 79.93°W) from 2014 to 2015. The observations were conducted using the leaves of the upper canopies of four tree species (red maple, bigtooth aspen, trembling aspen, and white ash) approximately every 10 days. In their measured data set, Rubisco content was not available. We used measured $Vcmax_{25}$ to invert Rubisco content. Combining Equations 2 and 6, the Rubisco content (g m^{-2}) R can be estimated as

$$R = \frac{55 \times V_{\max}^{25}}{8 \times 10^2 \left(c - d \times V_{\max}^{25}\right)}, \tag{12}$$

where $V_{\max}^{25}$ is the $Vcmax_{25}$ measured by Croft et al. (2017) and c and d were coefficients in Equation 6. Their values are 3.1 and 0.015 fitted with the data of birch reported by Laisk et al. (2005) and Eichelmann et al. (2004) (blue line in Figure S2).

The inverted Rubisco content was used to verify the relationship between chlorophyll and Rubisco contents and whether Equation 5 performed consistently in the wheat paddock and a temperate mixed deciduous forest.

2.9. Dummy Variable Regression Analysis

Dummy variable regression analysis (Gujarati, 1970) was used to test whether the regression coefficients of the linear relationship between chlorophyll and Rubisco were significantly different in the wheat paddock in China and the temperate mixed deciduous forest in Canada. First, the dummy variable was set to only 0 or 1 to identify subsets of observations (0 for wheat and 1 for forest). Then, a multiple linear regression model was built with Rubisco content as the dependent variable and three independent variables (chlorophyll content, dummy variable, and the product of the dummy variable and chlorophyll content) using the R language. The significance of individual coefficients of the multiple linear regression model was tested. If coefficients of dummy variable and the product of the dummy variable and chlorophyll content pass the significance test, the slope and intercept of the linear regression between chlorophyll and Rubisco contents are significantly different between the winter wheat and temperate mixed deciduous forest.

3. Results

3.1. Seasonal Variations in Leaf Rubisco and Other Biochemical Parameters

The seasonal dynamics of measured winter wheat Rubisco, chlorophyll, and nitrogen contents was assessed in order to investigate the temporal correlation of leaf biochemical constituents with Rubisco content and the partitioning of nutrient resources (Figure 1).

The leaf Rubisco content varied throughout the winter wheat growing season (Figure 1a). At the elongation stage, the Rubisco content of the top new leaves showed a downward trend. At the booting stage, the Rubisco content of the flag leaves gradually increased with leaf age until the flowering stage, reaching a peak of 2.74 g m^{-2}. Then, the Rubisco content declined rapidly at the filling stage. Leaf chlorophyll content had a similar temporal change as Rubisco. The maximum chlorophyll content also appeared around the flowering stage and began to decline after entering the filling stage. These results indicated that the temporal variations of leaf Rubisco and chlorophyll contents were consistent.

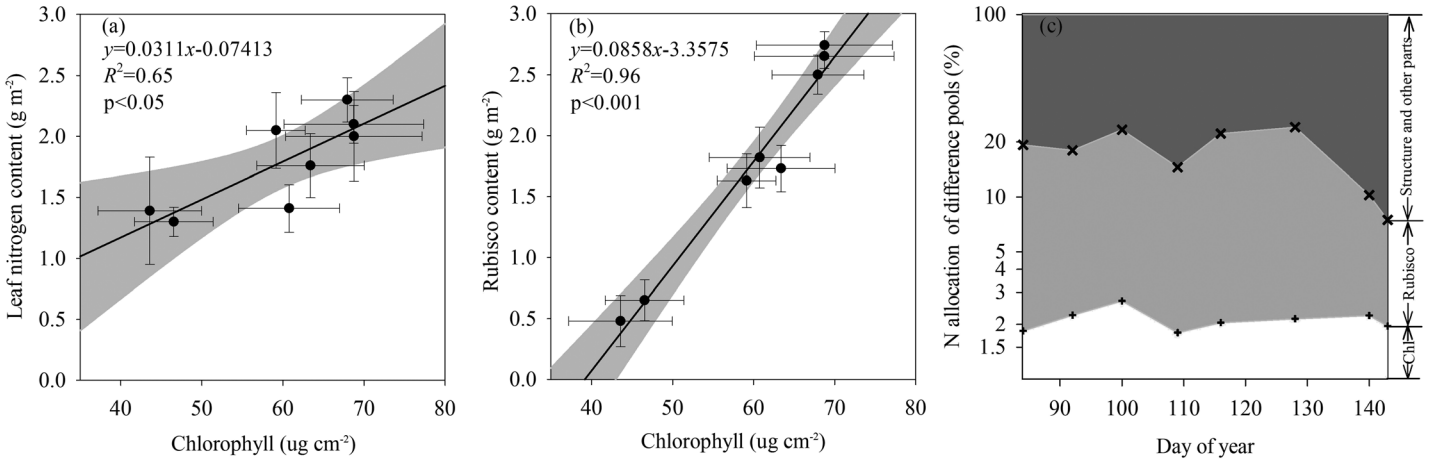

Figure 2. The relationship of leaf chlorophyll content (ug cm^{-2}) with (a) leaf nitrogen (g m^{-2}) and (b) Rubisco contents (g m^{-2}); and (c) is the variation of N partitioning among different N pools across the growing season of winter wheat. Horizontal error bars in (a) and (b) represent standard deviation of leaf chlorophyll content. Vertical error bars in (a) and (b) represent standard deviation of leaf nitrogen and Rubisco contents, respectively. The log scale of *y* axis was used in (c) for better visualization.

The change in leaf nitrogen content was inconsistent with the changes in Rubisco and chlorophyll contents. The peak of leaf nitrogen content appeared at the beginning and flowering stages of the growing season, which was different from the variations in both Rubisco and chlorophyll contents (Figures 1a and 1b). The dynamic changes in the nitrogen allocation to differential nitrogen pools can result in inconsistencies between the leaf nitrogen content and other plant traits, such as Rubisco and chlorophyll (Croft et al., 2017).

The seasonal variation of leaf $Vcmax_{25}$ (Figure 1c) was generally consistent with the changes in Rubisco and chlorophyll contents (Figure 1a). However, the obvious difference appeared at the anthesis stage of wheat (DOY 128). Observations at DOY 128 showed that measured $Vcmax_{25}$ clearly decreased after blooming, but both Rubisco and chlorophyll contents were still at high levels.

3.2. The Relationship Among the Leaf Rubisco, Nitrogen, and Chlorophyll Contents

Based on observations of multiple species, Evans (1989) reported the linear relationship between chlorophyll and leaf nitrogen contents, which was confirmed by our observations for the winter wheat throughout the growing season (Figure 2) ($R^2 = 0.65$; $p < 0.05$). The observations on DOYs 100 and 109 were outside of the 95% confidence intervals of the regression (Figure 2a). Figure 2c demonstrates obvious changes in nitrogen allocation into different pools on these 2 days. These changes in the investment of nitrogen into leaf chlorophyll affect the robustness of the linear relationship between chlorophyll and leaf nitrogen contents. Generally, cropping management, such as fertilization and irrigation, lessened the environmental constraints on the nitrogen partitioning, resulting in a relative stable allocation of nitrogen to chlorophyll during the growing season (Figure 2c). Therefore, leaf chlorophyll and nitrogen contents maintained a good linear relationship in our study.

Chlorophyll content showed a better linear relationship with Rubisco content than with leaf nitrogen content, as chlorophyll and Rubisco are more directly related to photosynthetic physiology. Chlorophyll content was able to explain 96% of variations in Rubisco content. As two important nitrogen pools in the photosynthetic system, the dynamic changes of nitrogen allocated to chlorophyll and Rubisco were coordinated (Figure 2c). Consequently, Rubisco content had a stronger linear relationship with leaf chlorophyll content than with leaf nitrogen content, which provides a physiological basis of using chlorophyll as a proxy of Rubisco in the Rubisco-based semimechanistic model estimating $Vcmax_{25}$.

3.3. Modeling $Vcmax_{25}$ by Leaf Rubisco Content

$Vcmax_{25}$ can be modeled from plant traits using four different methods, which are described in sections 2.6 and 2.7. Their performances in estimating $Vcmax_{25}$ are shown in Figure 3. The estimation of $Vcmax_{25}$ by its linear relationship with leaf nitrogen content had a large error (Figure 3a). $Vcmax_{25}$ was not estimated well

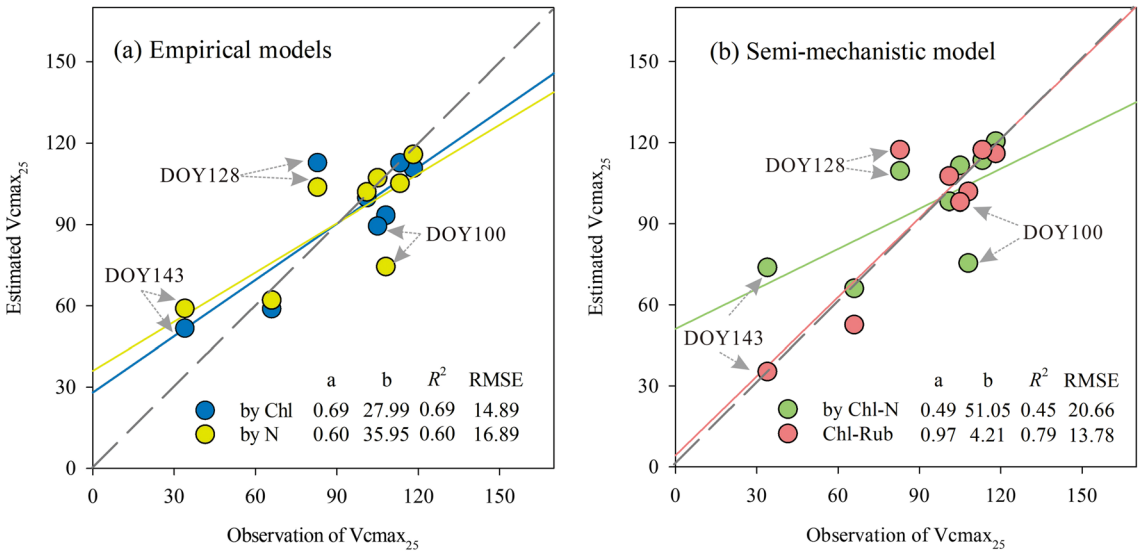

Figure 3. Comparing the observed $Vcmax_{25}$ with the estimated one of winter wheat by (a) linear relationship between $Vcmax_{25}$ and chlorophyll (blue circles) and between $Vcmax_{25}$ and nitrogen (yellow circles) and (b) semimechanistic models incorporating relationship between chlorophyll and nitrogen (Chl-N) contents (Houborg et al., 2013) (green circles) and relationship between chlorophyll and Rubisco contents established in this study (red circles).

using leaf nitrogen content in some days, such as DOYs 100 and 143, the nitrogen allocation changed evidently (Figure 2c). And on DOY 128, the modeled $Vcmax_{25}$ by leaf nitrogen content was also inconsistent with observation. Using chlorophyll content, which is one part of the photosynthetic nitrogen pool, the estimation of $Vcmax_{25}$ was improved in DOYs 100 and 143, except DOY 128.

As shown in Figure 3b, the semimechanistic model incorporating the relationship between chlorophyll and nitrogen contents (Houborg et al., 2013) performed the worst, greatly overestimating $Vcmax_{25}$ on DOYs 143 and DOY 140 during leaf senescence, due to its failure to properly consider the temporal change in nitrogen allocation between structural and photosynthetic fractions (Figure 2c). This model uses the empirical function reported by Evans (1989) to estimate Rubisco content according to total nitrogen content and a temporally invariant fraction of nitrogen allocated into Rubisco. Our semimechanistic model incorporating the relationship between chlorophyll and Rubisco contents had the best ability to model $Vcmax_{25}$ (Figure 3b), with a slope of 0.97 and an R^2 of 0.79. The best performance of this model is attributable to the better description of the nonlinear processes of Rubisco turnover rate and nitrogen allocation that determine $Vcmax_{25}$. However, our model also noticeably overestimated $Vcmax_{25}$ on DOY 128.

3.4. Exploring the Chl-Rub Relationship for Modeling $Vcmax_{25}$ in a Temperate Mixed Deciduous Forest

The study by Croft et al. (2017) provided observations of $Vcmax_{25}$ and leaf chlorophyll content of different tree species throughout the growing seasons in 2014 and 2015. We used their measurements to invert leaf Rubisco content with Equation 12. The change of inverted Rubisco content with measured chlorophyll content in this temperate mixed deciduous forest is shown in Figure 4a. The chlorophyll and Rubisco contents have a good exponential relationship throughout the growing seasons ($R^2 = 0.66$, $p < 0.001$) (red line in Figure 4a), and the linear relationship was also significant over the whole data set ($R^2 = 0.60$, $p < 0.001$) (blue line in Figure 4a).

In this forest, the chlorophyll content was below 35 $\mu g\ cm^{-2}$ (symbols with pink edges) at the beginning and end of the growing seasons. In our study, Rubisco was not measured during the leaf germination and senescence stages of the winter wheat. As to the main stages of the growing season, the slopes of the linear Chl-Rub relationship were 0.0858 and 0.071 ($g\ m^{-2}$ Rubisco $\mu g^{-1}\ cm^{-2}$ chlorophyll) for the winter wheat (Figure 2b) and temperate mixed deciduous forest (Figure 4a), respectively. The test using dummy variable regression analysis (Gujarati, 1970) indicated that the slopes and intercepts of the linear regression equations in these two ecosystems did not differ significantly. The p values were 0.591 for slopes and 0.158 for

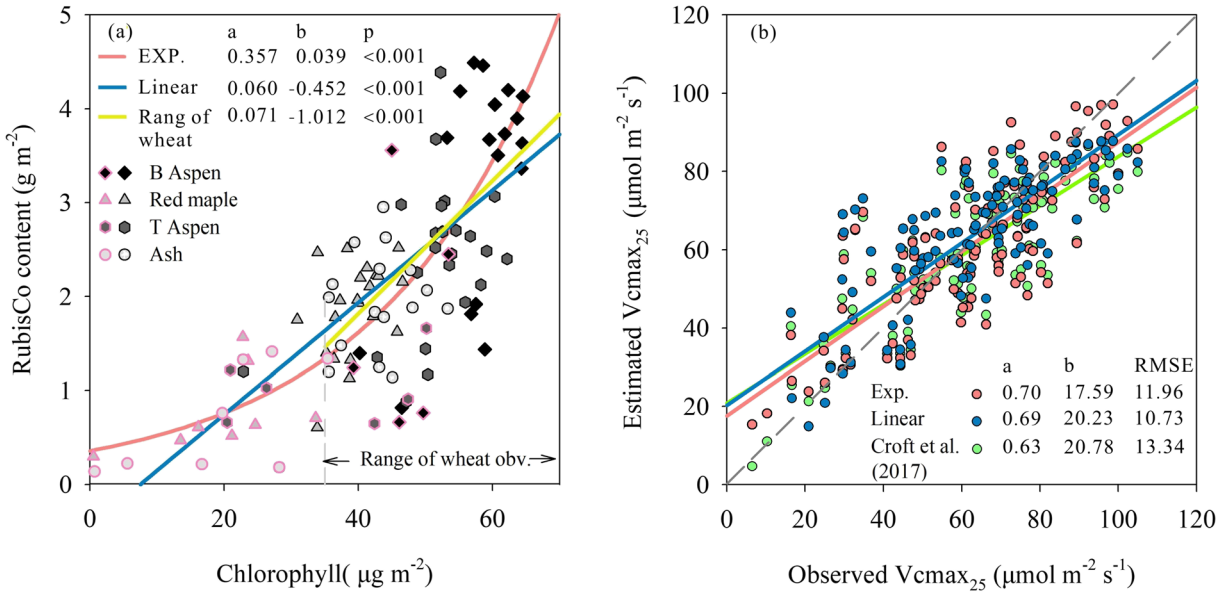

Figure 4. Relationship between measured chlorophyll and Rubisco estimated from measured $Vcmax_{25}$ using Equation 12 (a) and compassions of measured $Vcmax_{25}$ with estimates using different methods (b) in a temperate mixed deciduous forest during the growing seasons in 2014 to 2015. The dots with pink edges represented in (a) are the first or last two observations during individual growing seasons. In (b), red and blue circles are $Vcmax_{25}$ estimated using fitted exponential and linear Chl-Rub relationship, respectively. Green circles denote $Vcmax_{25}$ directly estimated from chlorophyll content (Croft et al., 2017). Exp. is the exponential function with the form $y = a\,(e^{bx})$. Linear is linear function with the form $y = ax + b$. ASH is white ash. B Aspen is bigtooth aspen. T Aspen is trembling aspen.

intercepts, indicating that a similar Chl-Rub relationship could be applied in these two different ecosystems at the main stage of the growing season.

$Vcmax_{25}$ was modeled using Equation 5 with Rubisco estimated using the measured chlorophyll content and fitted exponential and linear relationships (Figure 4a). $Vcmax_{25}$ modeled by the semimechanistic model developed in this study and estimated Rubisco content was closer to measured values than estimates directly using chlorophyll content in Croft et al. (2017) (Figure 4b). The root mean square errors (RMSEs) of $Vcmax_{25}$ estimated by exponential and linear functions of Chl-Rub were 11.96 and 10.73 μmol CO_2 m^{-2} s^{-1}, smaller than the RMSE of 13.34 μmol CO_2 m^{-2} s^{-1} in Croft et al. (2017). The slopes of regressions between observations and $Vcmax_{25}$ estimated using exponential and linear Chl-Rub relations were closer to 1.0 relative to that with $Vcmax_{25}$ estimated directly from chlorophyll content (Figure 4b). Thus, the Rubisco-based semimechanistic model (Equation 5) also improved the modeling of $Vcmax_{25}$ in this temperate mixed deciduous forest.

4. Discussion

4.1. Comparison of Different Ways to Model $Vcmax_{25}$ by Plant Traits

Previous studies have shown that $Vcmax_{25}$ could be well modeled by plant traits, including leaf nitrogen (N_{leaf}), Rubisco, chlorophyll, and specific leaf area (Croft et al., 2017; Dechant et al., 2017; Houborg et al., 2013; Miner & Bauerle, 2019; Walker et al., 2017; Watanabe et al., 2018). These models are difficult to apply to large scales because statistical relationships between plant traits and $Vcmax_{25}$ vary among species. For instance, the Chl-$Vcmax_{25}$ relationship was better than that of N_{leaf}-$Vcmax_{25}$ in a temperate mixed deciduous forest in Canada (Croft et al., 2017). A strong linear relationship of N_{leaf}-$Vcmax_{25}$ was reported in other ecosystems (Kattge et al., 2009; Walker et al., 2014). However, the slopes of the relationships of N_{leaf}-$Vcmax_{25}$ vary widely with species (Rogers et al., 2017).

The nitrogen in leaves can be roughly divided into structural and photosynthetic components (e.g., nitrogen in chlorophyll and Rubisco) (Evans, 1989). The ratio of nitrogen allocated in Rubisco to the total nitrogen in leaf varies among species (Ghimire et al., 2017). This ratio is also affected by environment (Liu et al., 2018)

and has seasonal variations (Croft et al., 2017; Miner & Bauerle, 2019). Therefore, accurate modeling of $Vcmax_{25}$ requires a factor that characterizes the fraction of the photosynthetic nitrogen. This factor is approximated by ratio of nitrogen allocated into Rubisco in Houborg et al. (2013) and leaf chlorophyll content in Croft et al. (2017).

As shown in Figure 3a, $Vcmax_{25}$ directly estimated using leaf nitrogen was largely different from the observations during the periods of flag leaf unfolding (DOY 100) and senescence (DOY143). The Chl-based linear model improved the estimates of $Vcmax_{25}$ on DOYs 100 and 143 since chlorophyll content characterized the dynamic of nitrogen in photosynthesis (Figure 2c). Rubisco is another important nitrogen pool in photosynthesis (Evans, 1989). Our measurements indicated a strong linear relationship between chlorophyll and Rubisco contents in a winter wheat system (Figure 2b). The model developed by Houborg et al. (2013) estimates $Vcmax_{25}$ according to nitrogen allocated in to Rubisco. Nitrogen content was estimated from chlorophyll content and used to determine the ratio of nitrogen allocated into Rubisco (Equations 9–11). Since two empirical functions were used (Equations 10 and 11), uncertainties might be accumulated. Based on the observed tight linkage between chlorophyll and Rubisco contents (Figures 2b and 4a), our model uses chlorophyll as the proxy of Rubisco and showed the best performance among four models, indicating the potential of chlorophyll content incorporated into the semimechanical model to map $Vcmax_{25}$ at regional and even global scales.

The model of Croft et al. (2017) is based on the linear relationship of Chl-$Vcmax_{25}$. The effect of Rubisco amount on $Vcmax_{25}$ was implicitly considered. Friend (1995) indicated that both the amount and turnover efficiency of Rubisco affect $Vcmax_{25}$. With turnover efficiency of Rubisco quantified using K_{cat}^{25}, our model considers the roles of these two factors in determining $Vcmax_{25}$. Therefore, it performed better than the model developed by Croft et al. (2017).

Our model also failed to estimate $Vcmax_{25}$ in some cases. To investigate whether the discrepancy between modeled and observed $Vcmax_{25}$ was caused by the uncertainties in Rubisco content estimated from chlorophyll content, $Vcmax_{25}$ was modeled using Equations 2 and 6 with measured Rubisco content as inputs. The R^2 and RMSE of modeled $Vcmax_{25}$ against observations were 0.72 and RMSE = 15.28 μmol CO_2 m^{-2} s^{-1} (Figure S3), indicating that uncertainties of modeled $Vcmax_{25}$ still exist even if measured Rubisco content was used. Equation 2 used to estimate $Vcmax_{25}$ assumes that all Rubisco are fully activated and $Vcmax_{25}$ changes consistently with Rubisco. It is not always the case. Evans and Clarke (2019) pointed out that part of Rubisco might be inactive and the ratio of active Rubisco to the total changes with environment and leaf age. Observations in tropical rainforest (Bahar et al., 2017), Arctic tundra (Rogers et al., 2017), and our study (DOY 128) demonstrated that $Vcmax_{25}$ derived from gas-exchange measurements were not always consistent with Rubisco content. In our study, the decoupling of Rubisco and $Vcmax_{25}$ in DOY 128 could be partially attributable to the low demand of CO_2 fixation in bloom stage (low $Vcmax_{25}$). The causes of this phenomenon are definitely worthy of further investigation. Nevertheless, the consideration of Rubisco activity in the Rubisco-based semimechanical model is a way for further improvement of $Vcmax_{25}$ estimation.

4.2. Variability of the Relationship Between Chlorophyll and Rubisco Contents With Vegetation Types

Observations during the rice growing season indicated that the degradation of Rubisco content was approximately 5 days earlier than that of chlorophyll content during leaf senescence (Ou et al., 2003). Due to the limitation of weather, our observations failed to capture the changes in Rubisco and chlorophyll contents during leaf senescence. The observed data of Croft et al. (2017), who conducted more measurements during leaf budding and senescence, showed that the exponential function was better in describing the relationship between Rubisco and chlorophyll contents than the linear function. Although the linear function was also able to capture the change of Rubisco with chlorophyll content at the significance level of 0.001 for both the winter wheat and temperate mixed deciduous forest (Figures 2 and 4), more measurements are required to fit the relationship of Rubisco with chlorophyll content for better applications of the semimechanistic model of $Vcmax_{25}$ in the different seasons over various ecosystems.

The content of chlorophyll is more related to $Jmax_{25}$, and the relationship between Rubisco and $Vcmax_{25}$ is more direct theoretically (Bonan, 2015; Sellers et al., 1992). The ratio of Jmax to Vcmax is affected by temperature (Medlyn et al., 2002), soil nutrients (Domingues et al., 2010; Kattge et al., 2009; Walker

et al., 2014), light (Hikosaka & Terashima, 1995; Niinemets et al., 1999), and genotype (Makino & Sage, 2007; Sudo et al., 2014). As shown in the study of Medlyn et al. (2002), the ratios of $Jmax_{25}$ to $Vcmax_{25}$ for crop and forest were different, implying that the correlation between chlorophyll and Rubisco contents might change with vegetation types to some extent.

Our research found that the Chl-Rub relationships of the winter wheat and temperate mixed deciduous forest were different but not significant. The temperate mixed deciduous forest was regrowth from farmland abandoned in the early twentieth century (Froelich et al., 2015), in which soil nitrogen is rich (McDonough & Watmough, 2015). The rich soil nitrogen of this forest might change the leaf Chl-Rub relationship and bring it close to that of the farmland ecosystem. Nevertheless, data from only two sites in this study are not enough to prove the consistent relationship between chlorophyll and Rubisco contents across vegetation types. More observational data of various vegetation types are required to verify the relationship.

4.3. Retrieval of $Vcmax_{25}$ From Rubisco With Remote Sensing Data

Vegetation reflectance in the red edge (700–760 nm) band and the green band is sensitive to chlorophyll content, which is the physical basis for retrieving chlorophyll content from remote sensing data (Datt, 1999; Gitelson et al., 1996). Currently, leaf chlorophyll content can be retrieved using vegetation indices (Xu et al., 2019), canopy and leaf radiative transfer models (Croft et al., 2015; Houborg et al., 2013), and machine learning methods (Verrelst et al., 2012). Successful retrieval of chlorophyll content from remote sensing data makes it possible to map $Vcmax_{25}$ at large scales. Of course, there are still considerable uncertainties in remotely sensed chlorophyll content (Croft et al., 2020). Improvement on the retrieval of chlorophyll content from remote sensing data will enhance the applicability of mapped $Vcmax_{25}$ by TBMs.

Previous studies have shown that remotely sensed chlorophyll content could be used to map $Vcmax_{25}$ at a large scale according to the statistical relationships of chlorophyll content with Vcmax (Croft et al., 2017) and nitrogen content (Houborg et al., 2013). However, these relationships change with plant species and are affected by environmental factors (Croft et al., 2017; Zhang et al., 2014). Our research found relatively consistent linear relationship between leaf chlorophyll and Rubisco contents in the winter wheat and temperate mixed deciduous forest. Chlorophyll content could be an effective proxy of Rubisco content for estimating $Vcmax_{25}$. However, even if the Rubisco content is well simulated, the current Rubisco-based semimechanistic model still cannot simulate $Vcmax_{25}$ well in some cases due to without consideration of changes in Rubisco activity. If Chl-Rub relationship is supported by more observations in different ecosystems under various environments and the Rubisco-based semimechanistic model is improved to capture the change in Rubisco activity, $Vcmax_{25}$ might be mapped from remotely sensed chlorophyll content at regional and global scales. The spatially and temporally variant $Vcmax_{25}$ data would be helpful for constraining uncertainties of TBMs, which currently fix $Vcmax_{25}$ or empirically adjust this key parameter according to simulated leaf nitrogen content (Medvigy et al., 2013; Walker et al., 2017).

5. Conclusions

In this study, the relationship between chlorophyll and Rubisco contents was established using observations throughout the growing season from a winter wheat paddock in China. This relationship was incorporated into a Rubisco-based semimechanistic model to simulate $Vcmax_{25}$. The robustness of this relationship was examined by observed chlorophyll content and inverted Rubisco content in a temperate mixed deciduous forest, Canada. Our results indicated that the correlation between chlorophyll and Rubisco contents was strong ($R^2 = 0.96$) for the winter wheat because the absorption of light energy by chlorophyll and the amount of CO_2 catalyzed by Rubisco were tightly coupled. In the semimechanistic model, both leaf Rubisco content and Rubisco turnover rate were quantified by the intimate Chl-Rub relationship, which made the simulated $Vcmax_{25}$ closer to observations than those modeled by two empirical correlation models and a semimechanistic model simulating $Vcmax_{25}$ from nitrogen content estimated from chlorophyll content. The slope of the Chl-Rub relationship was relatively consistent in the winter wheat and temperate mixed deciduous forest. If the Chl-Rub relationship is confirmed by more observations, remotely sensed chlorophyll content could be used as a proxy of Rubisco content for better mapping spatially and temporally continuous $Vcmax_{25}$, and the reduction of uncertainty in global carbon budget estimation is expected.

Appendix A: Calculation of K_{cat}^{25}

K_{cat}^{25} is calculated by reorganization of Equation 2:

$$K_{cat}^{25} = \frac{550,000 V_{max}^{25} \times 10^{-6}}{8 \times R}, \quad \text{(A1)}$$

where K_{cat}^{25} is the Rubisco turnover rate at 25°C (mol CO_2 mol sites^{-1} s^{-1}); V_{max}^{25} is the $Vcmax_{25}$ (μmol CO_2 m^{-2} s^{-1}); and R is leaf RuBisCo content (g m^{-2}).

Data Availability Statement

All the data underlying the findings of this article can be accessed in the DRYAD repository (https://datadryad.org/stash/share/XRkqaQ1eJYedRKDfpIOpBMo6PxdUx_6WWbSTOI2LOck).

Acknowledgments
Financial support for the study was provided by the National Key R&D Program of China (2016YFA0600202) and the National Natural Science Foundation of China (41871334). We are grateful for constructive comments from reviewers and editors, which are very helpful for improving the quality of our manuscript.

References

Allen, J. F. (2002). Photosynthesis of ATP—Electrons, proton pumps, rotors, and poise. *Cell*, *110*(3), 273–276. https://doi.org/10.1016/S0092-8674(02)00870-X

Anav, A., Friedlingstein, P., Beer, C., Ciais, P., Harper, A., Jones, C., et al. (2015). Spatiotemporal patterns of terrestrial gross primary production: A review. *Reviews of Geophysics*, *53*(3), 785–818. https://doi.org/10.1002/2015RG000483

Andersson, I., & Backlund, A. (2008). Structure and function of Rubisco. *Plant Physiology and Biochemistry*, *46*(3), 275–291. https://doi.org/10.1016/J.PLAPHY.2008.01.001

Bahar, N. H. A., Hayes, L., Scafaro, A. P., Atkin, O. K., & Evans, J. R. (2018). Mesophyll conductance does not contribute to greater photosynthetic rate per unit nitrogen in temperate compared with tropical evergreen wet-forest tree leaves. *New Phytologist*, *218*(2), 492–505. https://doi.org/10.1111/nph.15031

Bahar, N. H. A., Ishida, F. Y., Weerasinghe, L. K., Guerrieri, R., O'Sullivan, O. S., Bloomfield, K. J., et al. (2017). Leaf-level photosynthetic capacity in lowland Amazonian and high-elevation Andean tropical moist forests of Peru. *New Phytologist*, *214*(3), 1002–1018. https://doi.org/10.1111/nph.14079

Beerling, D. J., & Quick, W. P. (1995). A new technique for estimating rates of carboxylation and electron transport in leaves of C3 plants for use in dynamic global vegetation models. *Global Change Biology*, *1*(4), 289–294. https://doi.org/10.1111/j.1365-2486.1995.tb00027.x

Bernacchi, C. J., Singsaas, E. L., Pimentel, C., Portis, A. R. Jr., & Long, S. P. (2001). Improved temperature response functions for models of Rubisco-limited photosynthesis. *Plant, Cell and Environment*, *24*(2), 253–259. https://doi.org/10.1111/j.1365-3040.2001.00668.x

Bonan, G. (2015). *Ecological climatology: Concepts and applications*. Cambridge: Cambridge University Press.

Bonan, G. B., & Doney, S. C. (2018). Climate, ecosystems, and planetary futures: The challenge to predict life in Earth system models. *Science*, *359*(6375), eaam8328. https://doi.org/10.1126/science.aam8328

Bonan, G. B., Lawrence, P. J., Oleson, K. W., Levis, S., Jung, M., Reichstein, M., et al. (2011). Improving canopy processes in the Community Land Model version 4 (CLM4) using global flux fields empirically inferred from FLUXNET data. *Journal of Geophysical Research*, *116*(G2), G02014. https://doi.org/10.1029/2010JG001593

Burns, R. A., MacDonald, C. D., McGinn, P. J., & Campbell, D. A. (2005). Inorganic carbon repletion disrupts photosynthetic acclimation to low temperature in the cyanobacterium Synechococcus elongatus. *Journal of Phycology*, *41*(2), 322–334. https://doi.org/10.1111/j.1529-8817.2005.04101.x

Croft, H., Chen, J. M., Luo, X., Bartlett, P., Chen, B., & Staebler, R. M. (2017). Leaf chlorophyll content as a proxy for leaf photosynthetic capacity. *Global Change Biology*, *23*(9), 3513–3524. https://doi.org/10.1111/gcb.13599

Croft, H., Chen, J. M., Wang, R., Mo, G., Luo, S., Luo, X., et al. (2020). The global distribution of leaf chlorophyll content. *Remote Sensing of Environment*, *236*, 111479. https://doi.org/10.1016/j.rse.2019.111479

Croft, H., Chen, J. M., Zhang, Y., Simic, A., Noland, T. L., Nesbitt, N., & Arabian, J. (2015). Evaluating leaf chlorophyll content prediction from multispectral remote sensing data within a physically-based modelling framework. *ISPRS Journal of Photogrammetry and Remote Sensing*, *102*, 85–95. https://doi.org/10.1016/j.isprsjprs.2015.01.008

Datt, B. (1999). Visible/near infrared reflectance and chlorophyll content in Eucalyptus leaves. *International Journal of Remote Sensing*, *20*(14), 2741–2759. https://doi.org/10.1080/014311699211778

Dechant, B., Cuntz, M., Vohland, M., Schulz, E., & Doktor, D. (2017). Estimation of photosynthesis traits from leaf reflectance spectra: Correlation to nitrogen content as the dominant mechanism. *Remote Sensing of Environment*, *196*, 279–292. https://doi.org/10.1016/J.RSE.2017.05.019

Domingues, T. F., Meir, P., Feldpausch, T. R., Saiz, G., Veenendaal, E. M., Schrodt, F., et al. (2010). Co-limitation of photosynthetic capacity by nitrogen and phosphorus in West Africa woodlands. *Plant, Cell & Environment*, *33*(6), 959–980. https://doi.org/10.1111/j.1365-3040.2010.02119.x

Duursma, R. A. (2015). Plantecophys—An R package for analysing and modelling leaf gas exchange data. *PLoS ONE*, *10*(11), e0143346. https://doi.org/10.1371/journal.pone.0143346

Eichelmann, H., Oja, V., Rasulov, B., Padu, E., Bichele, I., Pettai, H., et al. (2004). Development of leaf photosynthetic parameters in Betula pendula Roth leaves: Correlations with photosystem I density. *Plant Biology*, *6*(3), 307–318. https://doi.org/10.1055/s-2004-820874

Eichelmann, H., Talts, E., Oja, V., Padu, E., & Laisk, A. (2009). Rubisco *in planta* k_{cat} is regulated in balance with photosynthetic electron transport. *Journal of Experimental Botany*, *60*(14), 4077–4088. https://doi.org/10.1093/jxb/erp242

Evans, J. R., & Poorter, H. (2001). Photosynthetic acclimation of plants to growth irradiance: The relative importance of specific leaf area and nitrogen partitioning in maximizing carbon gain. *Plant, Cell and Environment*, *24*(8), 755–767. https://doi.org/10.1046/j.1365-3040.2001.00724.x

Evans, J. R. (1989). Photosynthesis and nitrogen relationships in leaves of C_3 plants. *Oecologia*, *78*(1), 9–19. https://doi.org/10.1007/BF00377192

Evans, J. R., & Clarke, V. C. (2019). The nitrogen cost of photosynthesis. *Journal of Experimental Botany*, *70*(1), 7–15. https://doi.org/10.1093/jxb/ery366

Farquhar, G. D., von Caemmerer, S., & Berry, J. A. (1980). A biochemical model of photosynthetic CO_2 assimilation in leaves of C_3 species. *Planta*, *149*(1), 78–90. https://doi.org/10.1007/BF00386231

Friedlingstein, P., Andrew, R. M., Rogelj, J., Peters, G. P., Canadell, J. G., Knutti, R., et al. (2014). Persistent growth of CO_2 emissions and implications for reaching climate targets. *Nature Geoscience*, *7*(10), 709–715. https://doi.org/10.1038/ngeo2248

Friend, A. D. D. (1995). PGEN: An integrated model of leaf photosynthesis, transpiration, and conductance. *Ecological Modelling*, *77*(2–3), 233–255. https://doi.org/10.1016/0304-3800(93)E0082-E

Froelich, N., Croft, H., Chen, J. M., Gonsamo, A., & Staebler, R. M. (2015). Trends of carbon fluxes and climate over a mixed temperate-boreal transition forest in southern Ontario, Canada. *Agricultural and Forest Meteorology*, *211-212*, 72–84. https://doi.org/10.1016/j.agrformet.2015.05.009

Ghimire, B., Riley, W. J., Koven, C. D., Kattge, J., Rogers, A., Reich, P. B., & Wright, I. J. (2017). A global trait-based approach to estimate leaf nitrogen functional allocation from observations. *Ecological Applications*, *27*(5), 1421–1434. https://doi.org/10.1002/eap.1542

Gitelson, A. A., Merzlyak, M. N., & Lichtenthaler, H. K. (1996). Detection of red edge position and chlorophyll content by reflectance measurements near 700 nm. *Journal of Plant Physiology*, *148*(3–4), 501–508. https://doi.org/10.1016/S0176-1617(96)80285-9

Groenendijk, M., Dolman, A. J., van der Molen, M. K., Leuning, R., Arneth, A., Delpierre, N., et al. (2011). Assessing parameter variability in a photosynthesis model within and between plant functional types using global Fluxnet eddy covariance data. *Agricultural and Forest Meteorology*, *151*(1), 22–38. https://doi.org/10.1016/j.agrformet.2010.08.013

Gujarati, D. (1970). Use of dummy variables in testing for equality between sets of coefficients in two linear regressions: A note. *American Statistician*, *24*(1), 50–52. https://doi.org/10.1080/00031305.1970.10477181

Hall, D. O., & Rao, K. K. (1999). *Photosynthesis* (pp. 1–214). Cambridge: Cambridge University Press.

Hikosaka, K. (2014). Optimal nitrogen distribution within a leaf canopy under direct and diffuse light. *Plant, Cell & Environment*, *37*(9), 2077–2085. https://doi.org/10.1111/pce.12291

Hikosaka, K., & Terashima, I. (1995). A model of the acclimation of photosynthesis in the leaves of C_3 plants to sun and shade with respect to nitrogen use. *Plant, Cell & Environment*, *18*(6), 605–618. https://doi.org/10.1111/j.1365-3040.1995.tb00562.x

Houborg, R., Cescatti, A., Migliavacca, M., & Kustas, W. P. (2013). Satellite retrievals of leaf chlorophyll and photosynthetic capacity for improved modeling of GPP. *Agricultural and Forest Meteorology*, *177*(1), 10–23. https://doi.org/10.1016/j.agrformet.2013.04.006

Kattge, J., Knorr, W., Raddatz, T., & Wirth, C. (2009). Quantifying photosynthetic capacity and its relationship to leaf nitrogen content for global-scale terrestrial biosphere models. *Global Change Biology*, *15*(4), 976–991. https://doi.org/10.1111/j.1365-2486.2008.01744.x

Keenan, T. F., & Williams, C. A. (2018). The terrestrial carbon sink. *Annual Review of Environment and Resources*, *43*(1), 219–243. https://doi.org/10.1146/annurev-environ-102017-030204

Knyazikhin, Y., Schull, M. A., Stenberg, P., Mõttus, M., Rautiainen, M., Yang, Y., et al. (2013). Hyperspectral remote sensing of foliar nitrogen content. *Proceedings of the National Academy of Sciences of the United States of America*, *110*(3), E185–E192. https://doi.org/10.1073/pnas.1210196109

Krall, J. P., & Edwards, G. E. (1992). Relationship between photosystem II activity and CO2 fixation in leaves. *Physiologia Plantarum*, *86*(1), 180–187. https://doi.org/10.1111/j.1399-3054.1992.tb01328.x

Laisk, A., Eichelmann, H., Oja, V., Rasulov, B., Padu, E., Bichele, I., et al. (2005). Adjustment of leaf photosynthesis to shade in a natural canopy: Rate parameters. *Plant, Cell and Environment*, *28*(3), 375–388. https://doi.org/10.1111/j.1365-3040.2004.01274.x

Le Quéré, C., Andrew, R. M., Friedlingstein, P., Sitch, S., Pongratz, J., Manning, A. C., et al. (2017). Global carbon budget 2017. *Earth System Science Data Discussions*, 1–79. https://doi.org/10.5194/essd-2017-123

Li, W., Ciais, P., Wang, Y., Yin, Y., Peng, S., Zhu, Z., et al. (2018). Recent changes in global photosynthesis and terrestrial ecosystem respiration constrained from multiple observations. *Geophysical Research Letters*, *45*(2), 1058–1068. https://doi.org/10.1002/2017GL076622

Liu, N., Wu, S., Guo, Q., Wang, J., Cao, C., & Wang, J. (2018). Leaf nitrogen assimilation and partitioning differ among subtropical forest plants in response to canopy addition of nitrogen treatments. *Science of the Total Environment*, *637-638*(1026–1034), 1026–1034. https://doi.org/10.1016/J.SCITOTENV.2018.05.060

Makino, A., Mae, T., & Chira, K. (1986). Colorimetric measurement of protein stained with Coomassie Brilliant Blue R on sodium dodecyl sulfate–polyacrylamide gel electrophoresis by eluting with formamide. *Agricultural and Biological Chemistry*, *50*(7), 1911–1912. https://doi.org/10.1080/00021369.1986.10867672

Makino, A., Mae, T., & Ohira, K. (1985). Photosynthesis and ribulose-1,5-bisphosphate carboxylase/oxygenase in rice leaves from emergence through senescence. Quantitative analysis by carboxylation/oxygenation and regeneration of ribulose 1,5-bisphosphate. *Planta*, *166*(3), 414–420. https://doi.org/10.1007/BF00401181

Makino, A., & Sage, R. F. (2007). Temperature response of photosynthesis in transgenic rice transformed with “sense” or “antisense” rbcS. *Plant and Cell Physiology*, *48*(10), 1472–1483. https://doi.org/10.1093/pcp/pcm118

Markwell, J., Osterman, J. C., & Mitchell, J. L. (1995). Calibration of the Minolta SPAD-502 leaf chlorophyll meter. *Photosynthesis Research*, *46*(3), 467–472. https://doi.org/10.1007/BF00032301

McDonough, A. M., & Watmough, S. A. (2015). Impacts of nitrogen deposition on herbaceous ground flora and epiphytic foliose lichen species in southern Ontario hardwood forests. *Environmental Pollution*, *196*, 78–88. https://doi.org/10.1016/j.envpol.2014.09.013

Medlyn, B. E., Dreyer, E., Ellsworth, D., Forstreuter, M., Harley, P. C., Kirschbaum, M. U. F., et al. (2002). Temperature response of parameters of a biochemically based model of photosynthesis. II. A review of experimental data. *Plant, Cell and Environment*, *25*(9), 1167–1179. https://doi.org/10.1046/j.1365-3040.2002.00891.x

Medvigy, D., Jeong, S. J., Clark, K. L., Skowronski, N. S., & Schäfer, K. V. R. (2013). Effects of seasonal variation of photosynthetic capacity on the carbon fluxes of a temperate deciduous forest. *Journal of Geophysical Research, Biogeosciences*, *118*(4), 1703–1714. https://doi.org/10.1002/2013JG002421

Miner, G. L., & Bauerle, W. L. (2019). Seasonal responses of photosynthetic parameters in maize and sunflower and their relationship with leaf functional traits. *Plant, Cell & Environment*, *42*(5), 1–14. https://doi.org/10.1111/pce.13511

Niinemets, Ü., Oja, V., & Kull, O. (1999). Shape of leaf photosynthetic electron transport versus temperature response curve is not constant along canopy light gradients in temperate deciduous trees. *Plant, Cell & Environment*, *22*(12), 1497–1513. https://doi.org/10.1046/j.1365-3040.1999.00510.x

Onoda, Y., Wright, I. J., Evans, J. R., Hikosaka, K., Kitajima, K., Niinemets, Ü., et al. (2017). Physiological and structural tradeoffs underlying the leaf economics spectrum. *New Phytologist*, *214*(4), 1447–1463. https://doi.org/10.1111/nph.14496

Ou, Z., Peng, C., Lin, G., & Yang, C. (2003). Relationship between PSII excitation pressure and content of Rubisco large subunit or small subunit in flag leaf of super high-yielding hybrid rice. *Acta Botanica Sinica*, *45*(8), 929–935.

Piao, S., Sitch, S., Ciais, P., Friedlingstein, P., Peylin, P., Wang, X., et al. (2013). Evaluation of terrestrial carbon cycle models for their response to climate variability and to CO_2 trends. *Global Change Biology*, *19*(7), 2117–2132. https://doi.org/10.1111/gcb.12187

Quebbeman, J. A., & Ramirez, J. A. (2016). Optimal allocation of leaf-level nitrogen: Implications for covariation of Vcmax and Jmax and photosynthetic downregulation. *Journal of Geophysical Research, Biogeosciences*, *121*(9), 2464–2475. https://doi.org/10.1002/2016JG003473

Rogers, A., Medlyn, B. E., Dukes, J. S., Bonan, G., von Caemmerer, S., Dietze, M. C., et al. (2017). A roadmap for improving the representation of photosynthesis in Earth system models. *New Phytologist*, *213*(1), 22–42. https://doi.org/10.1111/nph.14283

Rogers, A., Serbin, S. P., Ely, K. S., Sloan, V. L., & Wullschleger, S. D. (2017). Terrestrial biosphere models underestimate photosynthetic capacity and CO_2 assimilation in the Arctic. *New Phytologist*, *216*(4), 1090–1103. https://doi.org/10.1111/nph.14740

Sellers, P. J., Berry, J. A., Collatz, G. J., Field, C. B., & Hall, F. G. (1992). Canopy reflectance, photosynthesis, and transpiration. III. A reanalysis using improved leaf models and a new canopy integration scheme. *Remote Sensing of Environment*, *42*(3), 187–216. https://doi.org/10.1016/0034-4257(92)90102-P

Smith, N. G., Keenan, T. F., Prentice, I. C., Wang, H., Wright, I. J., Niinemets, Ü., et al. (2019). Global photosynthetic capacity is optimized to the environment. *Ecology Letters*, *22*(3), 506–517. https://doi.org/10.1111/ele.13210

Stinziano, J. R., Morgan, P. B., Lynch, D. J., Saathoff, A. J., McDermitt, D. K., & Hanson, D. T. (2017). The rapid A–C_i response: Photosynthesis in the phenomic era. *Plant, Cell & Environment*, *40*(8), 1256–1262. https://doi.org/10.1111/pce.12911

Sudo, E., Suzuki, Y., & Makino, A. (2014). Whole-plant growth and N utilization in transgenic rice plants with increased or decreased rubisco content under different CO_2 partial pressures. *Plant and Cell Physiology*, *55*(11), 1905–1911. https://doi.org/10.1093/pcp/pcu119

Verheijen, L. M., Brovkin, V., Aerts, R., Bönisch, G., Cornelissen, J. H. C., Kattge, J., et al. (2013). Climate of the past geoscientific instrumentation methods and data systems impacts of trait variation through observed trait-climate relationships on performance of an Earth system model: A conceptual analysis. *Biogeosciences*, *10*(8), 5497–5515. https://doi.org/10.5194/bg-10-5497-2013

Verrelst, J., Muñoz, J., Alonso, L., Delegido, J., Rivera, J. P., Camps-Valls, G., & Moreno, J. (2012). Machine learning regression algorithms for biophysical parameter retrieval: Opportunities for Sentinel-2 and -3. *Remote Sensing of Environment*, *118*(15), 127–139. https://doi.org/10.1016/J.RSE.2011.11.002

von Caemmerer, S., & Farquhar, G. D. (1981). Some relationships between the biochemistry of photosynthesis and the gas exchange of leaves. *Planta*, *153*(4), 376–387. https://doi.org/10.1007/BF00384257

Walker, A. P., Beckerman, A. P., Gu, L., Kattge, J., Cernusak, L. A., Domingues, T. F., et al. (2014). The relationship of leaf photosynthetic traits—V_{cmax} and J_{max}—to leaf nitrogen, leaf phosphorus, and specific leaf area: A meta-analysis and modeling study. *Ecology and Evolution*, *4*(16), 3218–3235. https://doi.org/10.1002/ece3.1173

Walker, A. P., Quaife, T., van Bodegom, P. M., De Kauwe, M. G., Keenan, T. F., Joiner, J., et al. (2017). The impact of alternative trait-scaling hypotheses for the maximum photosynthetic carboxylation rate (V_{cmax}) on global gross primary production. *New Phytologist*, *215*(4), 1370–1386. https://doi.org/10.1111/nph.14623

Watanabe, M., Hoshika, Y., Inada, N., & Koike, T. (2018). Photosynthetic activity in relation to a gradient of leaf nitrogen content within a canopy of Siebold's beech and Japanese oak saplings under elevated ozone. *Science of the Total Environment*, *636*(15), 1455–1462. https://doi.org/10.1016/j.scitotenv.2018.04.423

Wellburn, A. R. (1994). The spectral determination of chlorophylls a and b, as well as total carotenoids, using various solvents with spectrophotometers of different resolution. *Journal of Plant Physiology*, *144*(3), 307–313. https://doi.org/10.1016/S0176-1617(11)81192-2

Wolf, B. (1982). A comprehensive system of leaf analyses and its use for diagnosing crop nutrient status. *Communications in Soil Science and Plant Analysis*, *13*(12), 1035–1059. https://doi.org/10.1080/00103628209367332

Wullschleger, S. D. (1993). Biochemical limitations to carbon assimilation in C-3 plants: A retrospective analysis of the A/C-i curves from 109 species. *Journal of Experimental Botany*, *44*(5), 907–920. https://doi.org/10.1093/jxb/44.5.907

Xu, M., Liu, R., Chen, J. M., Liu, Y., Shang, R., Ju, W., et al. (2019). Retrieving leaf chlorophyll content using a matrix-based vegetation index combination approach. *Remote Sensing of Environment*, *224*, 60–73. https://doi.org/10.1016/J.RSE.2019.01.039

Zhang, Y., Guanter, L., Berry, J. A., Joiner, J., van der Tol, C., Huete, A., et al. (2014). Estimation of vegetation photosynthetic capacity from space-based measurements of chlorophyll fluorescence for terrestrial biosphere models. *Global Change Biology*, *20*(12), 3727–3742. https://doi.org/10.1111/gcb.12664

Zhang, Y., Guanter, L., Joiner, J., Song, L., & Guan, K. (2018). Spatially-explicit monitoring of crop photosynthetic capacity through the use of space-based chlorophyll fluorescence data. *Remote Sensing of Environment*, *210*, 362–374. https://doi.org/10.1016/j.rse.2018.03.031